INTERNATIONAL JOURNAL OF HYDROGEN ENERGY 47 (2022) 29648–29660

Available online at www.sciencedirect.com

ScienceDirect

journal homepage: www.elsevier.com/locate/he

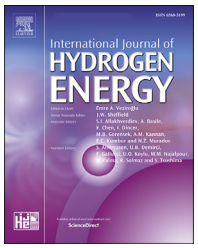

# Coordinate control law analysis for hydrogen blended electricity-gas integrated energy system

*Dengji Zhou* [a,b,*], *Xingyun Jia* [a], *Zhike Peng* [c,d], *Yushan Ma* [c]

[a] *The Key Laboratory of Power Machinery and Engineering of Education Ministry, Shanghai Jiao Tong University, Shanghai, 200240, PR China*

[b] *Sichuan Research Institute, Shanghai Jiao Tong University, Sichuan, 610213, PR China*

[c] *School of Mechanical Engineering, Ningxia University, Ningxia, 750021, PR China*

[d] *State Key Laboratory of Mechanical System and Vibration, Shanghai Jiao Tong University, Shanghai, 200240, PR China*

## HIGHLIGHTS

- Establish a dynamic hydrogen blended electricity-gas integrated system model.
- Solve the distribution parameter characteristics of the natural gas pipeline network.
- Dynamic simulation and verification of a real EG-IES in Central China was carried.
- Analysis of the different coordinate control performance during the load up process.

## ARTICLE INFO

*Article history:*
Received 5 May 2022
Received in revised form
18 June 2022
Accepted 27 June 2022
Available online 19 July 2022

*Keywords:*
Electricity-gas integrated energy system
Hydrogen blended natural gas pipeline network
Control law design
Dynamic characteristic

## ABSTRACT

Hydrogen-blended electricity-gas integrated energy system (EG-IES) utilizes surplus renewable energy power generation to blends hydrogen into the natural gas pipeline network for achieve efficient and economical large-scale hydrogen consumption and long-distance transportation. While enhancing the coupling between the power grid and gas grid, the scheduling control of such a complex system becomes increasingly important. The paper presents a dynamic model of a hydrogen blended EG-IES with high renewable energy permeability, and a modeling method that considers distribution parameters of the natural gas pipeline is obtained by using the cell segmentation and calculating the blended gas composition in real-time to avoid the assumption of constant composition. After the validation against available operational data, a case study of the certain area of Central China is simulated. The coordinate control law is reasonably designed according to the dynamic characteristics of EG-IES and the objective of realizing the load increase within the hydrogen concentration constraint, and the PID is utilized as the benchmark to compare dynamic performance. The results demonstrate that the coordinated control based on the alternate adjustment control law has no overshoot and shorter adjustment time of $p_l$ and $\varepsilon$ about 33% and 42% than benchmark on the large delay system.



* Correspondin author. The Key Laboratory of Power Machinery and Engineering of Education Ministry, Shanghai Jiao Tong University, PR China

E-mail address: zhoudj@sjtu.edu.cn (D. Zhou).

https://doi.org/10.1016/j.ijhydene.2022.06.274

## Introduction

Energy shortages and environmental pollution issues are impending due to the steady depletion of traditional fossil fuel reserves and the severity of the environmental pollution issues [1]. The transformation process of the global energy structure is accelerating, and many countries have carried out the development and utilization of renewable energy [1,2]. The uncertainty and discontinuity of renewable energy make it impossible to match user loads in real time, and the large-scale grid connection of a high proportion of renewable energy aggravates the contradiction between energy supply and demand in time and space [3]. The power-to-gas technology is an effective technology for absorbing surplus power generated by renewable energy, and it has a positive effect on optimizing the coupling between the power grid and the gas grid system [4]. Based on this background, the integrated energy system has become one of the effective technologies to solve the above problems because of its many advantages, such as considering the complementary coupling of multiple energy sources, fully absorbing renewable energy, and improving energy utilization [5].

Although the integrated energy system integrates multiple energy subsystems in the region, the shocks caused by an internal disturbance in a single energy subsystem are diffused and transmitted through various types of coupling elements as the degree of coupling between the energy subsystems increases, bringing significant uncertainty to the operation schedule. Especially in the typical electricity-gas integrated energy system (EG-IES), the tight coupling between the power grid system and the gas grid system makes the integrated energy system more complex [6]. Hydrogen blended natural gas pipeline network transportation is a technology that injects hydrogen from renewable energy sources such as wind and solar that cannot be balanced in real time into the natural gas pipeline network and distributes it efficiently to end users [7]. As of the end of 2020, the global natural gas consumption has reached 188.1 trillion cubic meters, and its share in primary energy rose to a record high of 24.7% [8]. International renewable energy agency reports in 2021 states that the total renewable energy generation capacity amounts to 3064 GW [9]. At present, there are much abandoned wind power and photovoltaic energy in renewable energy. If they are made into hydrogen and blended into the natural gas pipeline network for transportation, it can effectively reduce energy waste.

Although the hydrogen blended natural gas transportation improves energy utilization efficiency, it also enhances the coupling between the power grid and the gas grid, making the hydrogen-blended EG-IES model more complex. Therefore, in order to better analyze the characteristics of the system and provide a model basis for control scheduling, the modeling method of the hydrogen blended EG-IES becomes particularly important.

Cavana et al. [10] established an EG-IES dynamic simulation model to analyze the impact of hydrogen injection on the fluid dynamics and natural gas quality of natural gas networks under different scenarios. In the hydrogen blended EG-IES, the natural gas pipeline network system has the most significant change in the dynamic characteristics. Tabkhi et al. [11] established a dynamic model of the hydrogen blended natural gas pipeline network to study the characteristics of the mixed gas. Pan et al. [12] proposed a modeling method of electric-hydrogen integrated energy system by combining hydrogen production and storage technologies and considering the uncertainty of power generation load. Wang et al. [13] utilized the heat energy flow model under quality regulation and quantity regulation to simulate the dynamic thermal energy distribution, and used the pipeline heat conduction equation to reflect the real-time state of the pipeline. Zhou et al. [14] established the steady-state model of hydrogen blended EG-IES based on the real-scale natural gas pipeline network, renewable energy power generation and real user load, and analyzed the influence of hydrogen hybrid mode on the operation characteristics of natural gas pipeline network. Li et al. [15] designed an energy hub model to describe the energy conversion relationship dominated by electricity-heat-gas, and constructed a coupled model according to steady-state or transient characteristics. Chen et al. [16] proposed a comprehensive energy system modeling method considering the dynamic characteristics and uncertainties of wind power, and analyzed the dynamic characteristics of electricity, natural gas and heating systems with different time scales. Based on the multi-energy flow coupling calculation method of integrated energy system, Massure et al. [17] established an integrated energy system model of electricity-cooling-heating-gas. By separately calculating the coupling energy of the multi-energy flow, the thermal energy calculation speed of the integrated energy system is effectively improved, and the tight coupling of multi-energy flow is realized. Other similar integrated energy system dynamic modeling methods can be found in Refs. [18–20].

In addition, hydrogen blending brings new coupling effects and constraints to EG-IES with large inertial delay, and there are many methods for the conventional operation scheduling control of the integrated energy system. Li et al. [21] established a coordinated control framework for the multi-area integrated energy system using a multi-agent deep reinforcement learning method, and injected a variety of random disturbances to verify the reliability and effect of the algorithm. Guha et al. [22] proposed a cascaded fractional-order controller comprising three degrees of freedom proportional-integral-derivative and tilt-integral-derivative controllers for solving the load frequency control problems for an interconnected power system integrated with a doubly fed induction generator driven wind power generation system. In order to improve the performance of hybrid renewable energy system, Zhou et al. [23] developed a multi-objective optimal droop control strategy for the real-time power dispatch of the integrated energy system using Kirchhoff's law, and used a multi-objective genetic algorithm to optimize the control parameters. A model predictive control based robust scheduling strategy with a better adaptation to flexibility demands is proposed by Lv et al. [24] to maintain and utilize community integrated energy system flexibility for enhancing the uncertainty adaptability. Cheng et al. [25] proposed a multi-time scale coordinated optimization method of the integrated energy system with multi-energy flows and multi-type energy storage systems, and the optimization goal is to minimize its operation cost of a single day.

Considering multiple optimization objectives, Ershadi et al. [26] used genetic algorithm to conduct optimal scheduling research on the cooling-thermal power integrated energy system, considering the system economy, environmental protection and energy efficiency. Wang et al. [27] established an integrated energy system optimization model considering energy balance and external network transmission power, established an optimization objective function based on minimum cost, and performed steady-state optimal scheduling under multiple constraints. Wang et al. [28] studied the fault diagnosis and control method of dynamic process of integrated energy system based on machine learning. Yao et al. [29] established a dynamic optimal energy flow model for a thermoelectric integrated energy system, which integrated the transient temperature propagation effects in a district heating network based on a two-stage solution strategy. Zhang et al. [30] used a coupled network structure incorporating the thermodynamics-informed neural network and the compressor Boolean neural network to combine the functions of pipeline transportation safety inspection and energy supply prediction to construct an intelligent dispatch control for a hydrogen-blended natural gas plant. Yi et al. [31] proposed a distributed optimization control approach for the operation economy in an integrated energy system by considering various equality and inequality constraints to accommodate the integration of intermittent renewable generations. The proposed distributed neurodynamic-based control approach only requires the information exchange among neighboring units and offers flexibility and lower communication burden compared with some traditional centralized methods.

Through the analysis of the existing research, there are few researches on the coordinated control under the dynamic load up target of the hydrogen blended EG-IES with constraints. Most of the control methods are model-based and objective function-based, which do not consider the dynamic large inertial and coupling characteristics of hydrogen-blended EG-IES. In addition, some existing scheduling control methods of integrated energy system mainly use intelligent optimization algorithm to solve the objective optimization function. The strong coupling and large inertia characteristics of hydrogen blended EG-IES make it challenging to obtain real-time system feedback fluctuation through optimization control and attain the optimal objective of a strong nonlinear system in real time. Based on the above analysis, this study systematically proposed a coordinate control law design method for hydrogen blended EG-IES that account the dynamic characterises of the energy facilities. The innovations of this paper are as follows:

(1) This study establishes a hydrogen blended EG-IES high-fidelity dynamic model that considers the dynamic characteristics of coal-fired power plants, gas-fired power plants and natural gas pipelines, and the flow and pressure requirements of user nodes in dynamic test case simulation derived from the actual data on site. Hydrogen is produced from surplus renewable energy and blended into the natural gas pipeline system for transportation, which enhances the strong coupling between the power grid and the gas grid.
(2) This study utilizes the cell segmentation method with fine grain resolution to numerically solve the dynamic model of natural gas pipeline transportation with hydrogen blending that avoids the assumption of constant composition, and dynamic distribution parameters of natural gas pipelines by solving the real-time blending characteristics of gas components in each cell, which can provide more accurate observation values for production and operation scheduling. The dynamic blending properties of hydrogen and natural gas in time and space can be calculated based on the cell segmentation, and the method has a certain versatility to solve the blending of other gases.
(3) Under the condition of satisfying the hydrogen concentration constraint for hydrogen blended EG-IES load up control, the coordinate control laws are reasonably designed according to the large delay dynamic characteristics of the system, and the performance indicators of three different coordinate control methods are compared to provide a guarantee for the safe operation of the hydrogen blended EG-IES. Note that this work uses the PID controller as the benchmark.

## Hydrogen blended EG-IES dynamic modeling and simulation

The dynamic characteristics of hydrogen blended EG-IES is mainly reflected in coal-fired power plants, gas-fired power plants and hydrogen blended natural gas pipeline networks. In addition, unlike the power grid system with its small inertia and quick adjustment characteristics, the hydrogen blended natural gas pipeline network has a large system inertia. This section introduces the dynamic modeling of hydrogen blended EG-IES from the perspective of the power grid and gas grid system, including three modules: coal-fired power plant model, gas-fired power plant model, and hydrogen blended natural gas pipeline network model.

### *Power grid system*

#### *Coal-fired power plant model*

During the actual operation, the boiler-steam turbine unit in a coal-fired power plant is a nonlinear system with multiple inputs and outputs coupled with each other, which is mainly composed of direct-blown pulverizing systems, drum boilers and primary reheating condensing steam turbines [32]. The steam generated by coal combustion drives the steam turbine to generate electricity. In a hydrogen blended EG-IES, the dynamic model of a coal-fired power plant can be simplified as a second-order time delay system with coal consumption as input and power generation as output:

$$G_{coal}(s) = \frac{K_c e^{-\tau s}}{A_c s^2 + B_c s + 1} \tag{1}$$

where $A_c$, $B_c$ and $K_c$ are coefficients of the second-order system in the coal-fired power plant, $\tau$ is the time constant.

#### *Gas-fired power plant model*

As part of the current power system, gas-fired power plants play an important role in grid peak regulation and grid

security [33,34]. The dynamic model of gas-fired power plants in a hydrogen blended EG-IES can be simplified to a second-order system, and its input is the gas transmission volume and output is the power generation:

$$G_{gas}(s)=\frac{K_g}{A_g s^2+B_g s+1} \tag{2}$$

where $A_g$, $B_g$ and $K_g$ are coefficients of the second-order system in the gas-fired power plant.

Power generation from coal-fired power plants and gas-fired power plants cannot always meet the electrical load in real time due to the actual dynamic response delay, so the insufficient part needs to be balanced by the power grid. A balance node in the power grid is one where the voltage amplitude and phase remain constant and active and reactive power are injected, which can provide the system with the missing power.

The dynamic model parameters of coal-fired power plants and gas-fired power plants can be obtained through system identification based on historical operation data. The relevant basic parameters of power grid dynamic system are shown in Table 1.

**Table 1 – Basic parameters of the power grid system.**

| Symbol | $A_c$ | $B_c$ | $K_c$ | $\tau$ | $A_g$ | $B_g$ | $K_g$ |
|---|---|---|---|---|---|---|---|
| Value | 9107 | 243.5 | 8.7 | 0.4 | 0.01252 | 0.4502 | 17,017 |

### *Gas grid system*

The gas grid system in hydrogen blended EG-IES in this paper refers to the natural gas pipeline network [35], consisting mainly of natural gas pipelines and process equipment. The inertia of process equipment such as compressors and valves is much smaller than that of natural gas pipelines, so a steady-state model for process equipment is developed in this paper without considering their dynamic characteristics [36]. Hence, the dynamic model in the gas grid system mainly considers the dynamic characteristics of hydrogen blended natural gas pipelines.

#### *Hydrogen blended natural gas physical property calculation model*

Hydrogen blended with natural gas changes the physical properties of the mixed gas, and the calculation of each parameter is the basis for the dynamic simulation and scheduling of hydrogen blended transportation. The proportion of the mixed gas decreases with the hydrogen blending, reflecting in the improvement of the flow capacity in the transportation process and the higher compressor speed for pipeline network pressurization. Hence, the physical properties change of the mixed gas should be considered when establishing the dynamic model of the hydrogen blended natural gas pipeline.

The relationship between density $\rho$, pressure $p$ and temperature $T$ is constructed by using the actual gas state equation to calculate the physical properties of the mixed gas:

$$\begin{cases} p=\rho z R_g T \\ R_g=\dfrac{R}{M} \end{cases} \tag{3}$$

where $z$ is the compression factor of the mixed gas, $R_g$ is the gas constants, $R$ is the universal gas constant, and $M$ is the molar mass.

For the calculation of the compression factor $z_{mix}$ of the mixed gas, this paper adopts the formula proposed by the American Natural Gas Association to calculate [37]:

$$z_{mix}=1+\left(0.257-0.533\frac{T_{c,mix}}{T}\right)\frac{p}{p_{c,mix}} \tag{4}$$

where $T_{c,mix}$ and $p_{c,mix}$ are the pseudo-critical temperature and pressure of the mixture. When calculating the temperature and pressure of hydrogen and natural gas mixture, $T_{c,mix}$ and $p_{c,mix}$ are calculated according to the ideal mixing process [38], where the volume of the mixture is the sum of the volumes of hydrogen and natural gas. The calculation formulas for the $T_{c,mix}$ and $p_{c,mix}$ are:

$$T_{c,mix}=T_{c,H_2}\varepsilon+T_{c,ng}(1-\varepsilon) \tag{5}$$

$$p_{c,mix}=p_{c,H_2}\varepsilon+p_{c,ng}(1-\varepsilon) \tag{6}$$

where $\varepsilon$ is the volume fraction of hydrogen in the mixture, which also can be regarded as the hydrogen blending ratio, $T_{c,H_2}$ and $p_{c,H_2}$ are the pseudo-critical temperature and pressure of the hydrogen, $T_{c,ng}$ and $p_{c,ng}$ are the pseudo-critical temperature and pressure of the natural gas.

Besides, the coefficient of kinematic viscosity $\mu_{mix}$ of the mixture need to be calculated to solve the basic gas transportation equation:

$$\mu_{mix}=\frac{\mu_{H_2}\varepsilon\sqrt{M_{H_2}}+\mu_{ng}(1-\varepsilon)\sqrt{M_{ng}}}{\varepsilon\sqrt{M_{H_2}}+(1-\varepsilon)\sqrt{M_{ng}}} \tag{7}$$

where $\mu_{H_2}$ and $\mu_{ng}$ are the coefficients of kinematic viscosity of the hydrogen and natural gas, $M_{H_2}$ and $M_{ng}$ are the molar mass of the hydrogen and natural gas.

#### *Hydrogen blended natural gas pipeline model*

EG-IES produces hydrogen from renewable energy, so the amount of hydrogen blended is directly determined by weather, grid capacity, and user load. These uncertainties bring great fluctuations to the temporal and spatial distribution of hydrogen concentration in the pipeline, so the dynamic model of hydrogen blended natural gas pipelines must consider the changes of equation parameters caused by changes in mixed gas composition to avoid the assumption of constant composition.

The flow of hydrogen blended natural gas in the pipeline follows the continuity equation, momentum equation and energy equation [39]:

$$\begin{cases} \dfrac{\partial\rho}{\partial t}+\dfrac{\partial(\rho v)}{\partial x}=0 \\ \dfrac{\partial(\rho v)}{\partial t}+\dfrac{\partial(\rho v^2+p)}{\partial x}+\dfrac{\lambda\rho v|v|}{2D}+\rho g\sin\theta=0 \\ q\rho A_{cs}dx=\dfrac{\partial}{\partial t}\left[(\rho A_{cs}dx)\left(c_v T+\dfrac{v^2}{2}+gz_h\right)\right] \\ +\dfrac{\partial}{\partial x}\left[(\rho v A_{cs}dx)\left(c_v T+\dfrac{p}{\rho}+\dfrac{v^2}{2}+gz_h\right)\right] \end{cases} \tag{8}$$

where $t$ represents the time, $x$ is the distance, $v$ is the transmission speed, $\lambda$ is the hydraulic friction coefficient, $D$ is the diameter of the pipeline, $g$ is the gravitational acceleration, $\theta$ is the angle between the pipeline and the horizontal plane, $q$ is the mass flow of the gas mixture, $A_{cs}$ is the cross-sectional area, $c_v$ is the constant volume specific heat capacity, and $z_h$ is the altitude. Note that the hydraulic friction coefficient $\lambda$ [40] is calculated by the relative roughness $\vartheta$ and Reynolds number $Re$:

$$\lambda = 0.067\left(2\vartheta + \frac{158}{Re}\right)^{0.2} \tag{9}$$

Assuming that the change of the altitude of the pipeline $(\theta = 0)$ and the temperature in the pipeline can be ignored, the one-dimensional isothermal flow equation of the horizontal pipeline can be simplified as:

$$\begin{cases} \dfrac{\partial \rho}{\partial t} + \dfrac{\partial(\rho v)}{\partial x} = 0 \\ \dfrac{\partial(\rho v)}{\partial t} + \dfrac{\partial(\rho v^2 + p)}{\partial x} + \dfrac{\lambda \rho v|v|}{2D} = 0 \end{cases} \tag{10}$$

Since the above partial differential equations cannot be solved analytically, the pipeline is divided into multiple cells of a given length $\Delta x$ and spatially discretized [41]. In each cell, it is assumed that the hydrogen concentration, pressure, and other physical parameters have no change in spatial distribution, and the mass flow is defined on the inlet and outlet sections of each cell [42], as shown on the left of Fig. 1. Finally, the hydrogen blended natural gas pipeline equation can be reduced to the form of an ordinary differential equation (ODE):

$$\begin{cases} \dfrac{\partial p}{\partial t} = -\alpha \Delta q \\ \dfrac{\partial q}{\partial t} = -\alpha \dfrac{2q}{p}\Delta q + \left(\alpha \dfrac{q^2}{p^2} - \dfrac{A_{cs}}{\Delta x}\right)\Delta p - \beta \dfrac{q^2}{p} \end{cases} \tag{11}$$

$$\alpha = \frac{z_{mix} R_g T}{A_{cs}\Delta x} \quad \beta = \lambda \frac{z_{mix} R_g T}{2 A_{cs} D}$$

where $\Delta q$ is the mass flow difference between the inlet and outlet of the cell, $\Delta p$ is the pressure difference between the front and rear cells. The independent variables of the simplified partial differential equation are $p$ and $q$, and $\alpha$ and $\beta$ are parameters related to gas physical properties in Eq. (11), which need to be updated and calculated in real time according to the change of mixed gas composition.

Hydrogen will flow alongside mainstream natural gas in the pipeline after being blended, so the contents of two adjacent cells will interact. The storage $V$ is defined as the total mass of the gas in the cell. For the $i$-th cell $(i = 1, \ldots, n)$, the storage $V_{i,t}$ at time $t$ is:

$$V_{i,t} = V_{i,t-1} + q_{i,t}\Delta t - q_{i+1,t}\Delta t \tag{12}$$

where $q_{i,t}$ is the inlet mass flow rate of the $i$-th cell at time $t$.

The volume fraction of hydrogen in the mixture $\varepsilon_{i,t}$ of the $i$-th cell at time $t$ can be calculated from the compression factor $z_{mix}$ and the gas constant $R_g$ of the current mixed gas.

$$p_{i,t} = \rho_{i,t} z_{mix}(\varepsilon_{i,t}) R_g(\varepsilon_{i,t}) T \tag{13}$$

$$\rho_{i,t} = \frac{V_{i,t}}{A_{cs}\Delta x} \tag{14}$$

Assuming that the hydrogen blending only occurs at the inlet of the pipeline, and the user nodes draw gases at the outlet of the pipeline, it is necessary to consider the ideal blending with the injected hydrogen for the first cell. The mass flow is calculated in the last cell and then transferred to the next pipeline. Fig. 1 demonstrates the boundary conditions of a single pipeline and solution process of gas mixture calculation, and the distribution parameters of the pipeline can be obtained through the spatial discretization method. Note that the $Q_{H_2}$ represents the standard volume flow of the hydrogen blending amount.

### *Dynamic simulation process description*

The solving process of the hydrogen blended EG-IES dynamic model is shown in Fig. 2. At the beginning of the simulation, the power grid state parameters need to be initialized, including the electrical load of each user node, the installed capacity of each power plant, and the maximum active/reactive power generation. The power flow distribution with the smallest loss under the input of the power grid system is calculated by the optimal power flow (OPF) reactive power optimization [43]. According to the OPF distribution calculation results, the actual power generation of gas-fired power plants, coal-fired power plants and renewable energy power plants can be obtained. The insufficient power generation in the dynamic response is made up by balance nodes. At the same time, the surplus power generation part is used to electrolyze water to produce hydrogen to be blended with

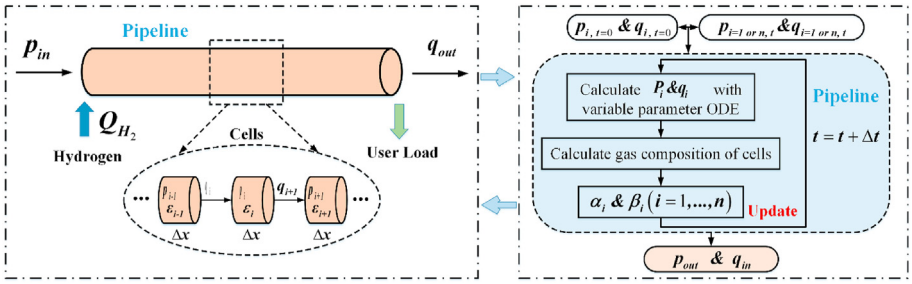


**Fig. 1 – Example of pipeline spatial discretization scheme and boundary conditions; schematic diagram of the solution process of hydrogen blended natural gas pipeline model.**

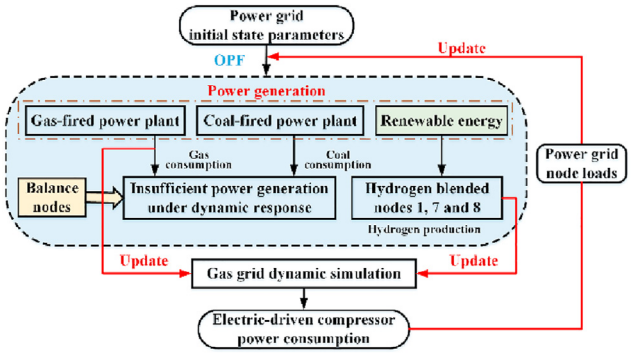


**Fig. 2 – Solving process of the hydrogen blended EG-IES dynamic model.**

nodes 1,7 and 8 in the natural gas pipeline network. The gas grid system simulation is carried out by updating the gas consumption of the gas-fired power plant, load demand and hydrogen blending amount of the hydrogen blended nodes. The power consumption of electric-driven compressor units obtained from the gas grid system simulation results will update parameters of the corresponding power grid load nodes, and then perform the next iteration to realize hydrogen blended EG-IES dynamic simulation process. Considering that the calculation of pipeline storage is involved in the dynamic model of hydrogen blended natural gas pipeline network, the simulation step in this paper is $\Delta t = 60s$ through optimal parameter tuning, which can not only meet the calculation requirements of the gas grid system, but also balance the running time of the hydrogen blended EG-IES.

## Result and discussion

### *Scene preset description and model validation*

The gas grid system simulation scenario of hydrogen blended EG-IES in this paper is the actual natural gas pipeline network in a certain area of Central China with 10-node. According to the actual electric load and grid scale of the area, the abstraction of the power grid system in the hydrogen blended EG-IES is simplified to IEEE39 node grid [44], as shown in Fig. 3. The power grid system includes 10 power generation nodes, including photovoltaic, wind, hydraulic, gas-fired and coal-fired power plants. The types and installed capacity of power plants and corresponding natural gas pipeline network nodes are shown in Table 2.

The power grid has 21 load nodes (residential and commercial load) [45]. Nodes 2, 5 and 13 of the gas grid system are electric-driven compressor units, and node 9 is a gas-turbine-driven compressor unit. Nodes 1, 4, 7, 8, 10, 11, and 12 of the EG-IES are user demand nodes. In addition, to take advantage of the surplus renewable energy, excess electricity is used to produce hydrogen and blend it into nodes 1, 7 and 8 of the natural gas pipeline networks. Note that the actual pipeline lengths, 24-h gas pipeline network inlet pressure and flow rate, renewable energy power generation and user load coefficients information of the hydrogen blended EG-IES scene in this paper can be found in Refs. [14,46].

In order to verify the hydrogen blended EG-IES dynamic model, this paper utilizes the real 24-h transient data of the outlet pressure $p_{l,real}$ and outlet mass flow $q_{l,real}$ in the lower line from the Chinese West-to-East Gas Pipeline to verify the simulation results of the model. The simulation data is obtained by inputting actual inlet pressure and flow, renewable energy power generation and user load coefficient into the natural gas pipeline network model. Table 3 lists the comparison results between the outlet pressure and outlet mass flow of simulation data ($p_{l,sim}, q_{l,sim}$) and field data in the lower line. The average error between the simulated data and the measured data for pressure is 1.912%, and the average error for flow is 2.312%. Noting that the overall average error is within an acceptable range and can be used for control scheduling optimization research.

### *Case study*

In the current operation of the natural gas pipeline network, the pressure in the pipeline that decreases with the flow direction is usually used as the control variable for the pipeline regulation operation, and the pipeline pressure gradient line is generally selected as the natural gas pipeline network regulation basis. Considering the blended hydrogen generated by the surplus renewable energy, the coupling of EG-IES is significantly enhanced and the energy flow is more complex. Therefore, the dynamic operation control of hydrogen-blended EG-IES needs to pay attention to the significant influence of large inertia and strong coupling characteristics of the system.

If the natural gas pipeline network needs to be boosted to meet the load requirements of distant user nodes, the current natural gas pipeline network generally adopts the method of adjusting the pressure ratio of compressor units to increase the pressure of the natural gas pipeline network. After blending hydrogen into the system for transportation, a sudden increase in the inlet pressure will lead to an increase of hydrogen blending ratio $\varepsilon$. During the process of adjusting the pressure ratio of the compressor units to increase the overall pressure of the natural gas pipeline network of the hydrogen blended EG-IES, it is necessary to consider the constraint of hydrogen concentration to ensure that the $\varepsilon$ is within the limits of the pipeline material. Considering the natural gas pipeline network transportation target at the outlet of the remote node, the lower line outlet pressure $p_l$ and $\varepsilon$ are selected as the controlled variables in this work. The compressor unit pressure ratio Pr is the main factor affecting the pressure of the natural gas pipeline network, and the secondary factor affecting the hydrogen concentration. The hydrogen blending amount $Q_{H_2}$ is the main factor affecting the hydrogen concentration, and the secondary factor affecting the pressure of the natural gas pipeline network. The coupling relationship between the $p_l$ and $\varepsilon$ determines that the hydrogen blended EG-IES must coordinately control the Pr and $Q_{H_2}$ to meet the pressure and concentration requirements at the same time.

In order to design and analysis the coordinated control law for the hydrogen blended EG-IES with the large inertia, this section compares the control effect of the traditional proportional-integral-derivative (PID) as the benchmark

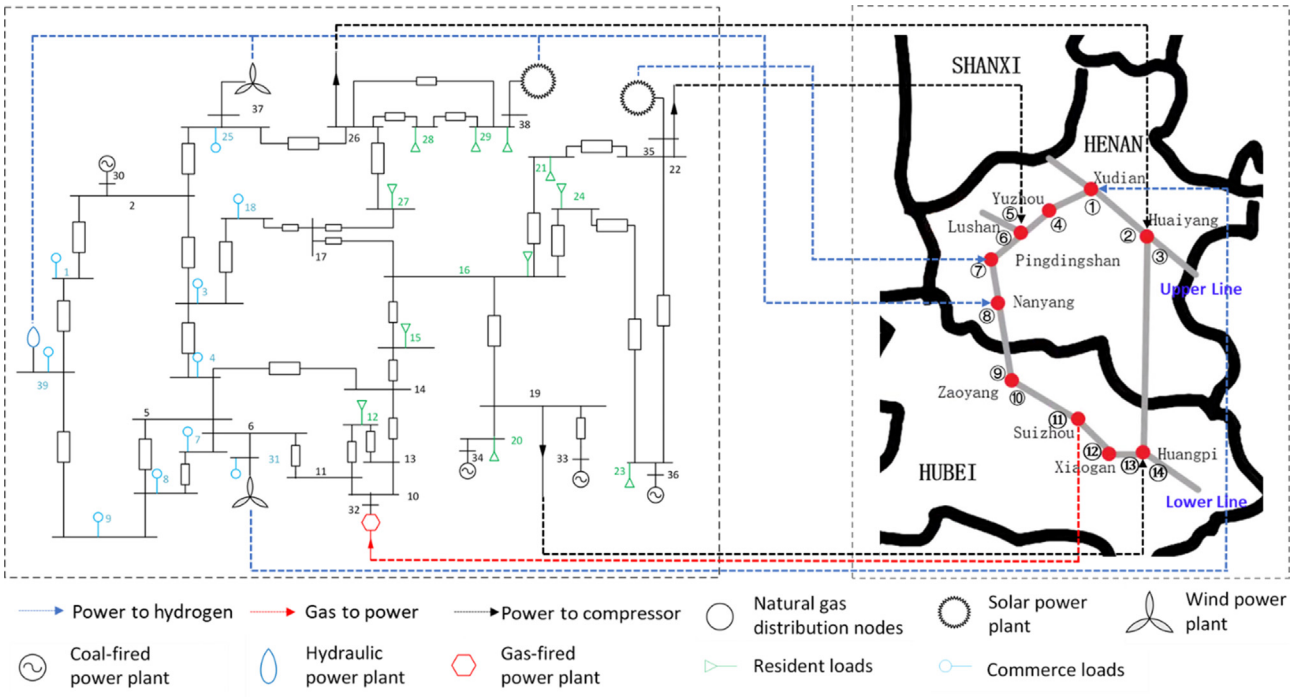


**Fig. 3 – Schematic diagram of hydrogen blended EG-IES.**

**Table 2 – Power plants and corresponding gas grid nodes.**

| Power plant nodes | Types | Installed capacity (MW) | Gas grid nodes |
|---|---|---|---|
| 30 | Coal-fired | 2600 | – |
| 31 | Wind | 99 | 1 |
| 32 | Gas-fired | 900 | 11 |
| 33 | Coal-fired | 2350 | – |
| 34 | Coal-fired | 2000 | – |
| 35 | Photovoltaic | 60 | 7 |
| 36 | Coal-fired | 2470 | – |
| 37 | Wind | 53.25 | 8 |
| 38 | Photovoltaic | 108 | 8 |
| 39 | Hydraulic | 1200 | 8 |

method to increase the lower line outlet pressure and reduce the outlet hydrogen blending ratio to meet the downstream demand control objective [47,48]. In this paper, the pressure ratio of the gas-driven compressor $Pr$ of lower line node 9 and the hydrogen blending amount $Q_{H_2}$ of the lower line node 7 are selected as the control quantities. When the hydrogen blending EG-IES is in a stable state, the control target is set to increase the lower line outlet pressure $p_l$ by 2 kPa, while the $\varepsilon$ is limited to 0.05. The following three cases compare the dynamic responses under the three coordinated control laws.

The *case 1* uses two PID controllers, the *case 2* uses a combination of the PID controller and a control law, and the *case 3* uses two alternating coordination control laws.

*Case 1: dynamic response of two PID controllers*

The hydrogen blended EG-IES is in a stable state at $2 \times 10^6$s, the $p_l$ of the lower line is 7.8274 MPa, and the $\varepsilon$ is 0.075. The first PID controller controls $Pr$ to achieve the goal of increasing $p_l$ by 2 kPa. The second PID controller controls $Q_{H_2}$ to reduce hydrogen blending ratio $\varepsilon$ to 0.05. Refer to refs [47] and [49], the control laws of two isomorphic PID controllers can be described as follows:

$$Pr(t) = K_{p1}\Delta p_l + K_{i1}\int \Delta p_l(t)dt + K_{d1}\dot{\Delta p}_l \tag{15}$$

$$Q_{H_2}(t) = K_{p2}\Delta\varepsilon + K_{i2}\int \Delta\varepsilon(t)dt + K_{d2}\dot{\Delta\varepsilon} \tag{16}$$

where, $K_p$ is the proportional coefficient, $K_i$ is the integral coefficient and $K_d$ is the differential coefficient. The subscript numbers indicate the controller sequence, 1 indicates the pressure loop controller, and 2 indicates the hydrogen blending amount loop controller. The inputs for the two PID controllers are the error $\Delta p_l$ and $\Delta\varepsilon$, which are the difference between the control signals and real feedback signals.

**Table 3 – Comparison Between Simulation Data and Field Data of Outlet Pressure and Outlet mass flow in the Lower Line.**

| Time | 03:00 a.m. | 06:00 a.m. | 09:00 a.m. | 12:00 p.m. | 15:00 p.m. | 18:00 p.m. | 21:00 p.m. | 24:00 p.m. | Average error |
|---|---|---|---|---|---|---|---|---|---|
| $p_{l,sim}$ (MPa) | 8.980 | 8.838 | 9.939 | 9.468 | 10.590 | 9.821 | 8.793 | 8.522 | 1.912% |
| $p_{l,real}$ (MPa) | 8.794 | 8.665 | 9.587 | 9.362 | 10.452 | 9.603 | 8.653 | 8.409 | |
| $q_{l,sim}$ (Kg/s) | 197.806 | 213.399 | 97.350 | 131.202 | 60.906 | 112.557 | 166.219 | 175.307 | 2.312% |
| $q_{l,real}$ (Kg/s) | 192.681 | 212.086 | 94.261 | 130.125 | 57.871 | 110.751 | 163.438 | 170.491 | |

According to the optimal parameter tuning, the gain coefficients of two PID controller are given in Table 4.

Fig. 4 and Fig. 5 demonstrate the dynamic trends of the control quantities *Pr* and $Q_{H_2}$. Fig. 6 and Fig. 7 show the dynamic response of the controlled quantities $p_l$ and $\varepsilon$. It can be seen from the above results that although the control objective is to increase the outlet pressure, the pressure ratio of the gas-driven compressor increases at first and then gradually decreases, and the final stable value is lower than that before the control. According to analysis, the reason for this phenomenon is that the hydrogen blending amount in the system is reduced, and a low hydrogen concentration will lead to an increase in pressure of the natural gas pipeline. As can be seen from Fig. 4, the *Pr* has experienced a process of increasing at first and then decreasing, so the overshoot of the outlet pressure in Fig. 6 is large, and the system needs about $8\times 10^5$s to reach the pressure setting target. Qualitative summary from dynamic response trend, setting a cooperative control strategy based on two PID controllers for two control objectives and control variables can achieve the established objectives. But influenced by the large inertia and strong coupling of the system itself, the dynamic response time is long, and the initial gradient of the compressor unit is opposite to the target direction, bringing extra loss.

*Case 2: dynamic response of a PID controller and a control law*

According to the control effect of *case 1*, the PID controller of the outlet pressure loop is reserved in *case 2*, and the parameter settings remain unchanged. The control law of the $Q_{H_2}$ shown in Fig. 9 is designed according to the final stabilization value and stabilization time in *case 1*. The pressure ratio control effect of the control method of the PID and control law coordinate control in *case 2* is shown in Fig. 8. And Fig. 10 shows the change of the outlet pressure of the lower line coordinate controlled by a PID controller and a designed control law. Compared with the *case 1*, the overshoot of the outlet pressure $p_l$ is reduced and the adjustment time is slightly shorter. Fig. 11 shows the change of the hydrogen blending ratio at the lower line outlet when the control law is used to control the $Q_{H_2}$ of node 7. The $\varepsilon$ is smoother, and the adjustment time of the $\varepsilon$ is about $6\times 10^5$s, which is shorter than PID control of the *case 1*. Overall, the coordinate control method using a PID controller and a control law reduces both the overshoot of the outlet pressure and the response time of the hydrogen blending ratio. However, the loss in the initial stage of the pressure ratio control law of the compressor unit still exists for about $1.3\times 10^5$s.

The purpose of this case is mainly to combine PID and control law for collaborative control. According to Fig. 5 in *case 1*, the design of the linear control law in Fig. 9 in this case is carried out. It can provide an intermediate benchmark for the coordinate control of two PIDs in *case1* and the coordinate control of two control laws in *case 3*. The dynamic response characteristics of Figs. 10 and 11 have obvious shape difference compared with Figs. 6 and 7, while the trend difference of the control command compared with Figs. 4 and 8 is small, which further proves the coupling influence of

**Table 4 – Parameters of the PID control.**

| Parameters | $K_p$ | $K_i$ | $K_d$ | $E_r$ |
|---|---|---|---|---|
| *Pr* PID | 0.012 | 0.006 | 0.007 | $\Delta p_l$ |
| $Q_{H_2}$ PID | 0.015 | 0.004 | 0.004 | $\Delta\varepsilon$ |

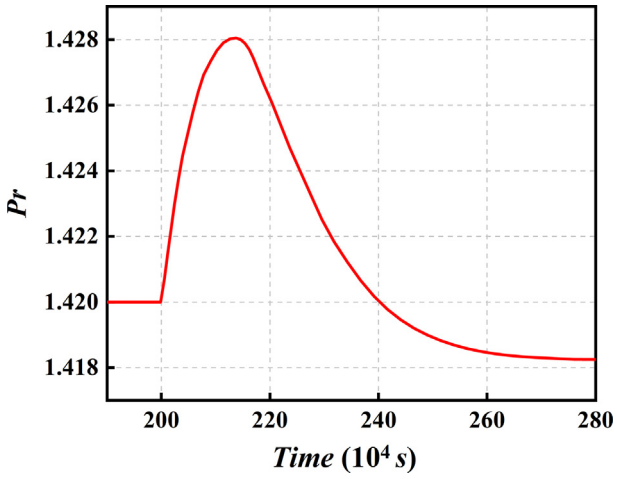


**Fig. 4 – Compressor pressure ratio *Pr* of the case 1.**

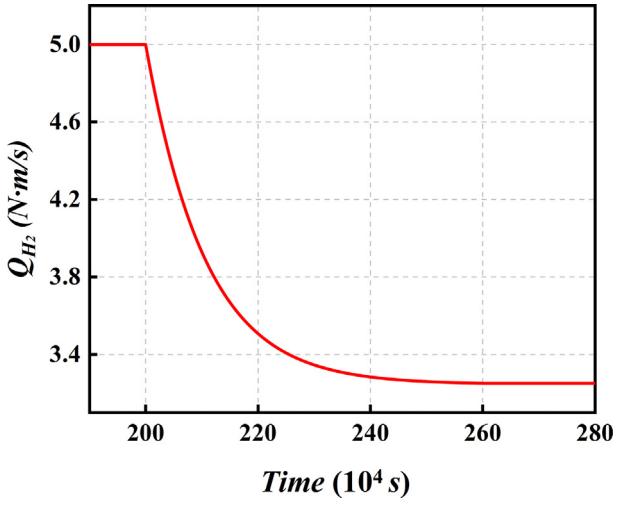


**Fig. 5 – Hydrogen blending amount $Q_{H_2}$ of the case 1.**

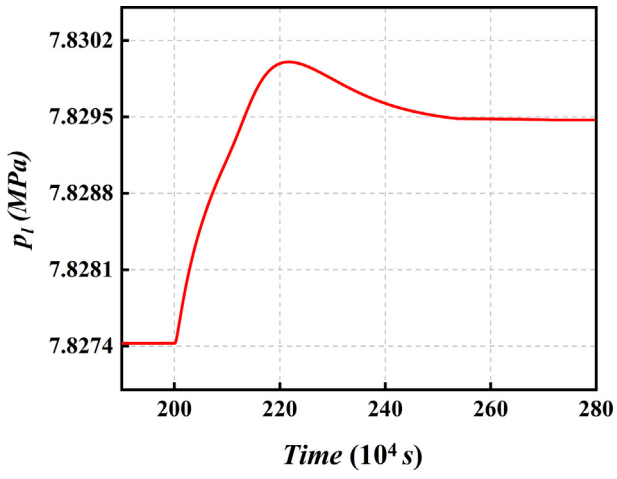


**Fig. 6 – Lower line outlet pressure $p_l$ of the case 1.**

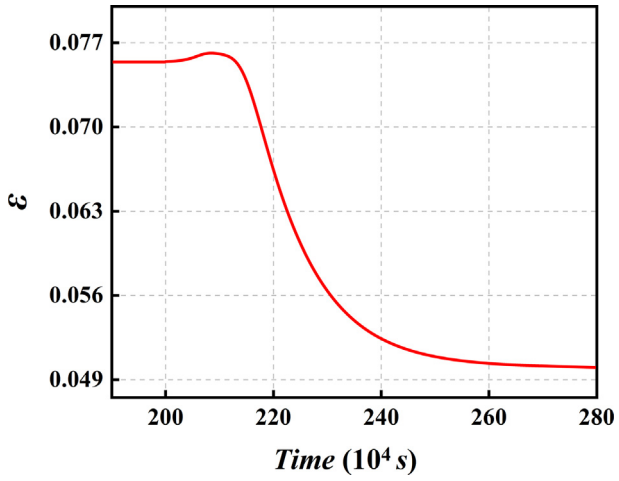


Fig. 7 – Hydrogen blending ratio $\varepsilon$ of the case 1.

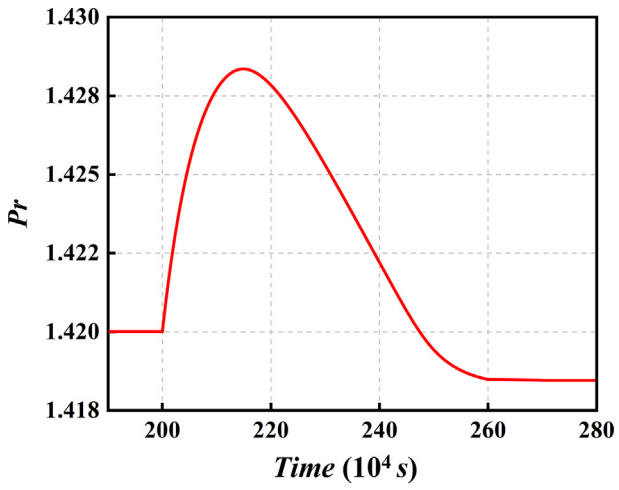


Fig. 8 – Compressor pressure ratio *Pr* of the case 2.

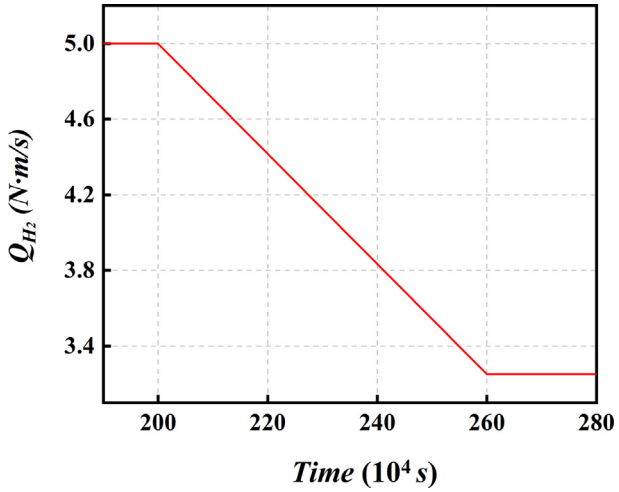


Fig. 9 – Hydrogen blending amount $Q_{H_2}$ of the case 2.

hydrogen blending amount on the dynamic characteristics of the natural gas pipeline.

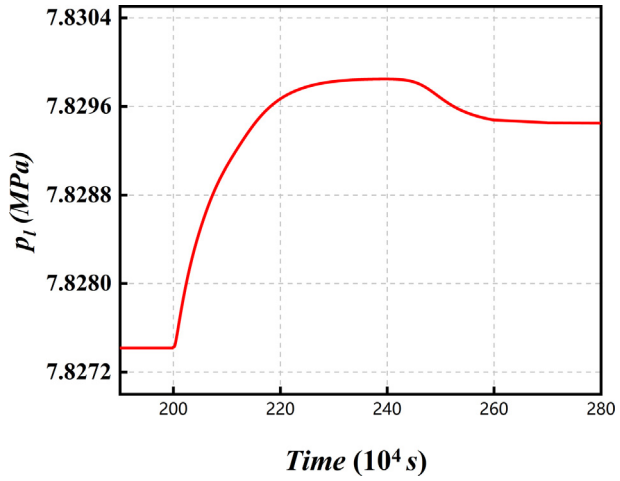


Fig. 10 – Lower line outlet pressure $p_l$ of the case 2.

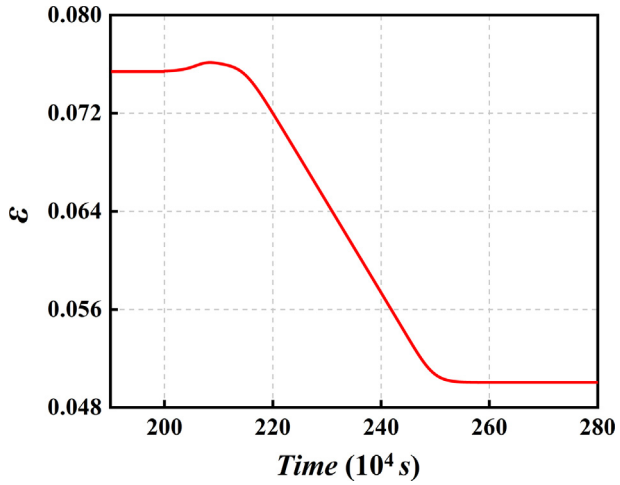


Fig. 11 – Hydrogen blending ratio $\varepsilon$ of the case 2.

*Case 3: dynamic response of coordination control law*

The coordinated control method of the *case 3* refers to designing the control law according to the dynamic characteristics to alternately control the pressure ratio of the gas-driven compressor and the hydrogen blending amount at node 7 to meet the outlet pressure requirement and the constraint of the outlet hydrogen blending ratio.

Since the compressor unit pressure ratio is the main factor affecting the outlet pressure of the natural gas pipeline network, the impact ratio $A_p$ of the pressure ratio on the outlet pressure is estimated with reference to the dynamic response of the outlet pressure when the *Pr* of the compressor suddenly decreases (shut down compressor unit). Based on the response of the outlet hydrogen blending ratio, the impact ratio $a_p$ of the pressure ratio on the outlet hydrogen blending ratio is estimated. At the same time, according to the response of the outlet hydrogen blending ratio when the surplus renewable energy power surges, the impact ratio $B_h$ of the hydrogen blending amount on the outlet hydrogen blending ratio is estimated, and the impact ratio $b_h$ of the hydrogen blending amount on the outlet pressure is estimated from the response of the lower line outlet pressure. Considering the

coupling factors of the pressure ratio of the compressor unit and the amount of hydrogen blending on the lower line outlet pressure and the hydrogen blending rate, the following coupling relationship is established:

$$\begin{cases} \Delta p = \Delta x_1 A_p + \Delta x_2 b_h \\ \Delta \varepsilon = \Delta x_2 B_h - \Delta x_1 a_p \end{cases} \tag{17}$$

where $\Delta p$ is the target increase of the outlet pressure, $\Delta\varepsilon$ is the target decrease of the outlet hydrogen blending ratio, $\Delta x_1$ is the change value of the outlet pressure, and $\Delta x_2$ is the change value of the outlet hydrogen blending ratio. The above variables are determined according to the minimum system variation of the hydrogen blended EG-IES under this control objective with the $\varepsilon$ constraint.

Based on the above principles, alternately control *Pr* and $Q_{H_2}$ three times, and the total adjustment time is $2 \times 10^5$s. The coordinated control law of alternate regulation in *case 3* is shown in Fig. 12. As can be seen from this figure, the red line control amount representing $Q_{H_2}$ is executed earlier than *Pr*, mainly to suppress the load-up phenomenon for boosting of the compressor unit in the initial stage. The changes of pressure and hydrogen blending rate in the initial stage are mainly controlled by the amount of hydrogen blending, ensuring the pressure target direction and the pressure ratio gradient direction are consistent in the subsequent stages, and reducing the internal loss of the hydrogen blended EG-IES.

Fig. 13 and Fig. 14 show the dynamic trends of the lower line outlet pressure and the hydrogen blending ratio during alternate adjustment coordinate control law of the *case 3*. Compared with the trend of dynamic response results in *case 1* and *case 2*, it has obviously better control effect. As can be seen from these figures, when the pressure ratio and the hydrogen blending ratio are controlled alternately, the system has almost no overshoot, and the adjustment time of the outlet pressure and the outlet hydrogen blending ratio are both about $4 \times 10^5$s, which is shortened by half compared with the adjustment time of *case 1*. Although the system has strong coupling nonlinearity, the alternating adjustment coordination control law designed in this paper achieves nearly linear control effect to a certain extent.

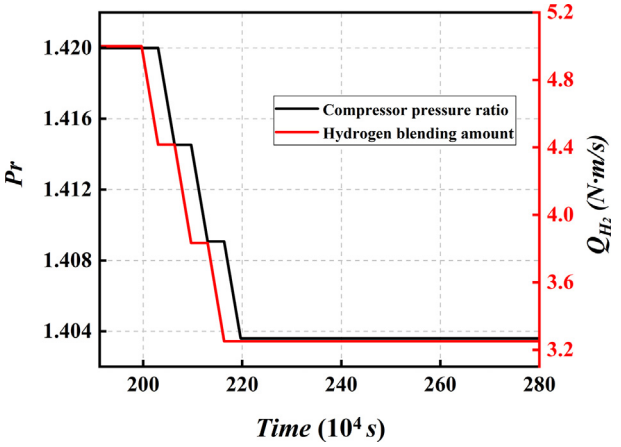


**Fig. 12 – Gas-driven compressor unit pressure ratio Pr and node 7 hydrogen blending amount $Q_{H_2}$ of the case 3.**

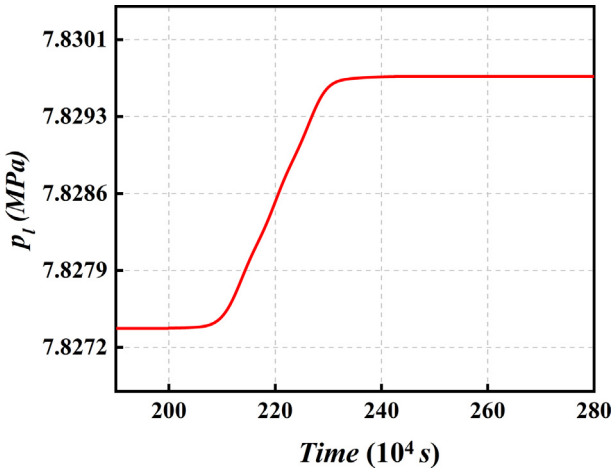


**Fig. 13 – Lower line outlet pressure $p_l$ of the case 3.**

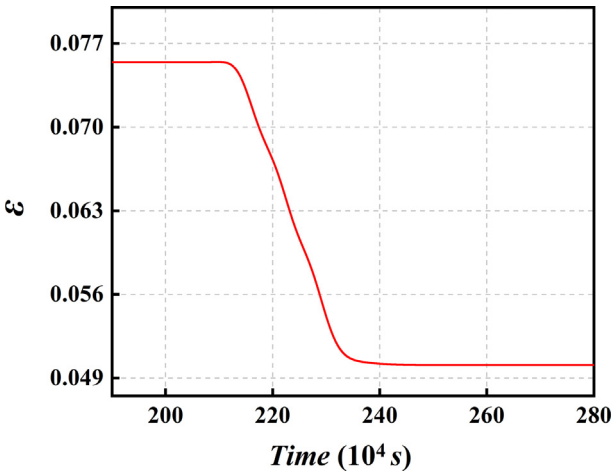


**Fig. 14 – Hydrogen blending ratio $\varepsilon$ of the case 3.**

*Method comparison*

Based on the respective simulation and analysis of the above three different cases, some qualitative conclusions can be drawn from the result figures. In order to quantitatively compare the control effects of the hydrogen-blended natural gas pipelines, this section mainly compares and analyzes some performance indicators of the dynamic response under the same control objective.

As listed in Table 5, four performance indicators of three different control methods are compared [50], including the overshoot of $p_l$, adjustment time of $p_l$, adjustment time of $\varepsilon$, and steady-state error of $p_l$. It can be seen from the table that the pressure steady-state control deviation of the PID control method is small, but the overshoot and adjustment time are

**Table 5 – Comparison of dynamic response performance indicators of different control methods.**

| Method | *Case 1* | *Case 2* | *Case 3* |
|---|---|---|---|
| Overshoot of $p_l$ (%) | 21.2 | 13.5 | **0** |
| Adjustment time of $p_l$ ($10^5$s) | 8 | 7 | **5** |
| Adjustment time of $\varepsilon$ ($10^5$s) | 8 | 6 | **4** |
| Steady-state error of $p_l$ ($10^{-4}$%) | **3.58** | 6.26 | 28.7 |

large. Note that the amount of overshoot in this paper is calculated based on the relative amount of the target setpoint and the initial state because of the pressure variable is smaller in magnitude than the pressure state. The coordinate control law of alternate adjustment method has almost no overshoot, and the adjustment time is very short, but the pressure steady-state control deviation is large. The adjustment time of $p_l$ of the *case 3* is the minimum value of $5 \times 10^5$s, which is an average of 33% lower than the rest of the cases. And the adjustment time of $\varepsilon$ of the *case 3* is the $4 \times 10^5$s, which is the minimum value and is an average of 42% lower than the other cases. At the same time, the steady-state error of $p_l$ of *case 3* is the largest, and that of *case 1* is the smallest. Based on the above analysis, in the coordinate control of the actual hydrogen blended EG-IES with large time delay, it is necessary to comprehensively consider the adjustment time and accuracy requirements, and choose the suitable system coordination control method to ensure system fast and accurate scheduling under the constraint of the safe operation.

## Conclusions

This research paper discussed the dynamic modeling of typical strongly coupled and nonlinear facilities of a hydrogen blended EG-IES in a certain area of Central China, including coal-fired power plants, gas-fired power plants, and the hydrogen blended natural gas pipeline network model. As for the single natural gas pipeline, the cell division method is applied to solve the pipeline transportation dynamic characteristic with hydrogen blended, and the hydrogen blended gas composition is recalculated in each cell and the parameters of the partial differential equation are updated that avoid the assumption of constant composition. Based on the control objective of realizing the load up of lower line under the condition of satisfying the hydrogen concentration constraint, the response effects of three cases of different coordinate control methods are designed and analyzed. In *case 1*, the pressure ratio and the hydrogen blending amount are controlled by two different PID controllers. In *case 2*, the pressure ratio is controlled by a PID controller, and the hydrogen blending amount is controlled by a control law based on the response results of *case 1*. *Case 3* is to design the coordinate control laws of the pressure ratio and hydrogen blending amount by means of alternate adjustment. And the main conclusions of the paper are as follows:

(1) The classical PID control method is used as the benchmark in the scheduling of EG-IES, and the results show that the adjustment time for such a system with large inertia is very long. In *case1* and *case 2*, the system adjustment time using the PID controller is $8\times 10^5$s and $7 \times 10^5$s respectively. And the PID controller has an integral term that can fully reduce the steady-state error and can achieve more accurate control. However, it is challenging to balance the relationship between the adjustment time and the overshoot of hydrogen blended EG-IES when using the PID controller to coordinate control, which makes the overshoot phenomenon appear in both *case 1* and *case 2* dynamic response effects.

(2) According to the designed alternate adjustment coordinate control law method of downstream outlet pressure and hydrogen incorporation rate, since it considers the dynamic response characteristics of hydrogen blended EG-IES, the phenomenon that the direction of the compressor operating condition and the actual target direction in the compared PID control method are reversed is effectively avoided. In addition to reducing the invalid loss of the system, the adjustment time and overshoot of the system are effectively reduced. The adjustment time of $p_l$ and $\varepsilon$ of the alternate adjustment coordinate control method in *case 3* is reduced by about 33% and 42%, respectively. According to the trend of the dynamic response results, although the hydrogen blended EG-IES has strong nonlinearity, the linearized response results can be achieved to a certain extent based on the alternate adjustment coordination control law in this paper.

(3) With the development of hydrogen blended EG-IES, it shows more and more complex changes in energy flow, working medium and conversion coupling, especially the complex changes in system spatial distribution and time brought about by the hydrogen blended transportation of natural gas pipeline network. The control effect of the energy storage system on the hydrogen blended EG-IES dynamic response can be considered in the subsequent control scheduling optimization research. In addition, with the continuous development of hydrogen blended EG-IES, intelligent control methods based on many real operation data can be developed.

## Declaration of competing interest

The authors declare that they have no known competing financial interests or personal relationships that could have appeared to influence the work reported in this paper.

## Acknowledgement

The authors appreciate the support from the Science and Technology Department of Ningxia (Grant No. 2022ZDYF1483), and Young Elite Scientists Sponsorship Program by CAST.

## REFERENCES

[1] Dosdoğru AT, İpek AÄB. Hybrid boosting algorithms and artificial neural network for wind speed prediction[J]. Int J Hydrogen Energy 2022;47(3):1449–60.
[2] Hansen K, Breyer C, Lund H. Status and perspectives on 100% renewable energy systems[J]. Energy 2019;175:471–80.
[3] Fu Y, Lin H, Ma C, et al. Effects of uncertainties on the capacity and operation of an integrated energy system[J]. Sustain Energy Technol Assessments 2021;48:101625.

[4] Sun W, Harrison GP, Dodds PE. A multi-model method to assess the value of power-to-gas using excess renewable[J]. Int J Hydrogen Energy 2022;47(15):9103–14.
[5] Arsad AZ, Hannan MA, Al-Shetwi AQ, et al. Hydrogen energy storage integrated hybrid renewable energy systems: a review analysis for future research directions[J]. Int J Hydrogen Energy 2022;47(39):17285–312.
[6] Escamilla A, Sánchez D, García-Rodríguez L. Assessment of power-to-power renewable energy storage based on the smart integration of hydrogen and micro gas turbine technologies[J]. Int J Hydrogen Energy 2022;47(40):17505–25.
[7] Kong M, Feng S, Xia Q, et al. Investigation of mixing behavior of hydrogen blended to natural gas in gas network[J]. Sustainability 2021;13(8):4255.
[8] Statistical review of world energy. https://www.bp.com/en/global/corporate/energy-economics/statistical-review-of-world-energy.html. [Accessed 28 April 2022].
[9] International renewable energy sAgency. https://www.irena.org/publications/2022/Apr/Renewable-Capacity-Statistics-2022. [Accessed 28 April 2022].
[10] Cavana M, Mazza A, Chicco G, et al. Electrical and gas networks coupling through hydrogen blending under increasing distributed photovoltaic generation[J]. Appl Energy 2021;290:116764.
[11] Tabkhi F, Azzaro-Pantel C, Pibouleau L, et al. A mathematical framework for modelling and evaluating natural gas pipeline networks under hydrogen injection[J]. Int J Hydrogen Energy 2008;33(21):6222–31.
[12] Pan G, Gu W, Lu Y, et al. Optimal planning for electricity-hydrogen integrated energy system considering power to hydrogen and heat and seasonal storage[J]. IEEE Trans Sustain Energy 2020;11(4):2662–76.
[13] Wang D, Zhi Y, Jia H, et al. Optimal scheduling strategy of district integrated heat and power system with wind power and multiple energy stations considering thermal inertia of buildings under different heating regulation modes[J]. Appl Energy 2019;240:341–58.
[14] Zhou D, Yan S, Huang D, et al. Modeling and simulation of the hydrogen blended gas-electricity integrated energy system and influence analysis of hydrogen blending modes [J]. Energy 2022;239:121629.
[15] Li R, Wei W, Mei S, et al. Participation of an energy hub in electricity and heat distribution markets: an MPEC approach [J]. IEEE Trans Smart Grid 2018;10(4):3641–53.
[16] Chen X, Wang C, Wu Q, et al. Optimal operation of integrated energy system considering dynamic heat-gas characteristics and uncertain wind power[J]. Energy 2020;198:117270.
[17] Massrur HR, Niknam T, Aghaei J, et al. Fast decomposed energy flow in large-scale integrated electricity–gas–heat energy systems[J]. IEEE Trans Sustain Energy 2018;9(4):1565–77.
[18] Uilhoorn FE. Dynamic behaviour of non-isothermal compressible natural gases mixed with hydrogen in pipelines[J]. Int J Hydrogen Energy 2009;34(16):6722–9.
[19] Ho A, Mohammadi K, Memmott M, et al. Dynamic simulation of a novel nuclear hybrid energy system with large-scale hydrogen storage in an underground salt cavern[J]. Int J Hydrogen Energy 2021;46(61):31143–57.
[20] Elaoud S, Hadj-Taïeb E. Transient flow in pipelines of high-pressure hydrogen–natural gas mixtures[J]. Int J Hydrogen Energy 2008;33(18):4824–32.
[21] Li J, Yu T, Zhang X. Coordinated load frequency control of multi-area integrated energy system using multi-agent deep reinforcement learning[J]. Appl Energy 2022;306:117900.
[22] Guha D, Roy PK, Banerjee S. Equilibrium optimizer-tuned cascade fractional-order 3DOF-PID controller in load frequency control of power system having renewable energy resource integrated[J]. Int Trans Electrical Energy Syst 2021;31(1):e12702.
[23] Zhou Y, Hua Q, Liu P, et al. Multi-objective optimal droop control of solid oxide fuel cell based integrated energy system[J]. Int J Hydrogen Energy 2022. https://doi.org/10.1016/j.ijhydene.2022.04.071. In press.
[24] Lv C, Yu H, Li P, et al. Model predictive control based robust scheduling of community integrated energy system with operational flexibility[J]. Appl Energy 2019;243:250–65.
[25] Cheng S, Wang R, Xu J, et al. Multi-time scale coordinated optimization of an energy hub in the integrated energy system with multi-type energy storage systems[J]. Sustain Energy Technol Assessments 2021;47(22):101327.
[26] Ershadi H, Karimipour A. Present a multi-criteria modeling and optimization (energy, economic and environmental) approach of industrial combined cooling heating and power (CCHP) generation systems using the genetic algorithm, case study: a tile factory[J]. Energy 2018;149:286–95.
[27] Wang Y, Wang Y, Huang Y, et al. Operation optimization of regional integrated energy system based on the modeling of electricity-thermal-natural gas network[J]. Appl Energy 2019;251:113410.
[28] Wang P, Poovendran P, Manokaran KB. Fault detection and control in integrated energy system using machine learning [J]. Sustain Energy Technol Assessments 2021;47:101366.
[29] Yao S, Gu W, Lu S, et al. Dynamic optimal energy flow in the heat and electricity integrated energy system[J]. IEEE Trans Sustain Energy 2020;12(1):179–90.
[30] Zhang T, Bai H, Sun S. Intelligent natural gas and hydrogen pipeline dispatching using the coupled thermodynamics-informed neural network and compressor boolean neural network[J]. Processes 2022;10(2):428.
[31] Yi Z, Xu Y, Hu J, et al. Distributed, neurodynamic-based approach for economic dispatch in an integrated energy system[J]. IEEE Trans Ind Inf 2019;16(4):2245–57.
[32] Bailera M, Lisbona P, Romeo LM. Avoidance of partial load operation at coal-fired power plants by storing nuclear power through power to gas[J]. Int J Hydrogen Energy 2019;44(47):26063–75.
[33] Nazir SM, Cloete S, Bolland O, et al. Techno-economic assessment of the novel gas switching reforming (GSR) concept for gas-fired power production with integrated CO2 capture[J]. Int J Hydrogen Energy 2018;43(18):8754–69.
[34] Huang D, Zhou D, Jia X, et al. A mixed integer optimization method with double penalties for the complete consumption of renewable energy in distributed energy systems[J]. Sustain Energy Technol Assessments 2022;52:102061.
[35] Zhou D, Huang D, Jia X, et al. Study on the maintenance scheduling model for compressor units of long-distance natural gas networks considering actual maintenance demands[J]. J Nat Gas Sci Eng 2021;94:104065.
[36] Zhou D, Huang D, Zhang L, et al. A global thermodynamic measurement data reconciliation model considering boundary conditions and parameter correlations and its applications to natural gas compressors[J]. Measurement 2021;172:108972.
[37] Iglesias-Silva GA, Hall KR. Natural gas compression factors calculated from relative density, heating value, and diluent compositions[J]. Chem Eng Technol: Industrial Chemistry-Plant Equipment-Process Engineering-Biotechnology 1996;19(5):467–72.
[38] Rakopoulos CD, Scott MA, Kyritsis DC, et al. Availability analysis of hydrogen/natural gas blends combustion in internal combustion engines[J]. Energy 2008;33(2):248–55.
[39] Alamian R, Behbahani-Nejad M, Ghanbarzadeh A. A state space model for transient flow simulation in natural gas pipelines[J]. J Nat Gas Sci Eng 2012;9:51–9.

[40] Ren H, Guo X, Yang J, et al. Selection of correlation parameters of friction coefficient in gas pipeline simulation [J]. Natural Gas and Oil 2013;14(5):418–25.
[41] Aalto H. Transfer functions for natural gas pipeline systems [J]. IFAC Proc Vol 2008;41(2):889–94.
[42] Guandalini G, Colbertaldo P, Campanari S. Dynamic modeling of natural gas quality within transport pipelines in presence of hydrogen injections[J]. Appl Energy 2017;185:1712–23.
[43] Longoria G, Lynch M, Curtis J. Green hydrogen for heating and its impact on the power system[J]. Int J Hydrogen Energy 2021;46(53):26725–40.
[44] Ufa RA, Malkova YY, Gusev AL, et al. Algorithm for optimal pairing of res and hydrogen energy storage systems[J]. Int J Hydrogen Energy 2021;46(68):33659–69.
[45] Zhou D, Ma S, Hao J, et al. An electricity load forecasting model for Integrated Energy System based on BiGAN and transfer learning[J]. Energy Rep 2020;6:3446–61.
[46] Zhou D, Ma S, Huang D, et al. An operating state estimation model for integrated energy systems based on distributed solution[J]. Front Energy 2020;14(4):801–16.
[47] Zhou D, Jia X, Hao J, Wang D, Huang D, Wei T. Study on intelligent control of gas turbines for extending service life based on reinforcement learning[J]. J Eng Gas Turbines Power 2021;143(6):61001.
[48] Conker C, Baltacioglu MK. Fuzzy self-adaptive PID control technique for driving HHO dry cell systems[J]. Int J Hydrogen Energy 2020;45(49):26059–69.
[49] Lee D, Cheon Y, Ryu JH, et al. An MCFC operation optimization strategy based on PID auto-tuning control[J]. Int J Hydrogen Energy 2017;42(40):25518–30.
[50] Jia X, Zhou D, Huang D, et al. Parametric analysis of variable stator vane system in gas turbines based on cosimulation of its refined model and system dynamic performance model[J]. Adv Theory Simulations 2021;4(12):2100286.

## Nomenclature

*Abbreviation*

*EG-IES:* Electricity-gas integrated energy system
*OPF:* Optimal power flow
*PID:* Proportional-integral-derivative
*ODE:* Ordinary differential equation

*Symbols*

$G_{coal}$: The transfer function of coal-fired power plant
$A_c, B_c, K_c$: Coefficients of the second-order system in the coal-fired power plant
$\tau$: The time constant
$G_{gas}$: The transfer function of gas-fired power plant
$A_g, B_g, K_g$: Coefficients of the second-order system in the gas-fired power plant
$p$: Pressure
$z$: Compression factor
$T$: Temperature
$R_g$: Gas constant
$R$: The universal gas constant
$M$: Molar mass
$z_{mix}$: The compression factor of the mixed gas
$T_{c,mix}$: The pseudo-critical temperature
$p_{c,mix}$: The pseudo-critical pressure
$\varepsilon$: The volume fraction of hydrogen in the mixture
$T_{c,H_2}$: The pseudo-critical temperature of the hydrogen
$p_{c,H_2}$: The pseudo-critical pressure of the hydrogen
$T_{c,ng}$: The pseudo-critical temperature of the natural gas
$p_{c,ng}$: The pseudo-critical pressure of the natural gas
$\mu_{mix}$: The kinematic viscosity coefficient of the gas mixture
$\mu_{H_2}$: The kinematic viscosity coefficient of the hydrogen
$\mu_{ng}$: The kinematic viscosity coefficient of natural gas
$M_{H_2}$: The molar mass of the hydrogen
$M_{ng}$: The molar mass of the natural gas
$t$: Time
$x$: Distance
$v$: The transmission speed
$\lambda$: The hydraulic friction coefficient
$D$: The diameter of the pipeline
$g$: The gravitational acceleration
$\theta$: The angle between pipeline and horizontal plane
$q$: Mass flow
$A_{cs}$: The cross-section area
$c_v$: The constant volume specific heat capacity
$z_h$: Altitude
$\vartheta$: The relative roughness
$Re$: Reynolds number
$\Delta x$: The length of cell
$\Delta q$: Mass flow difference
$\Delta p$: Pressure difference
$V_{i,t}$: The storage at time $t$ of i-th cell
$Q_{H_2}$: The standard volume flow of the hydrogen blending amount
$p_{l,sim}$: Simulation data of the lower line outlet pressure
$p_{l,real}$: Field data of the lower line outlet pressure
$q_{l,sim}$: Outlet mass flow simulation data of the lower line
$q_{l,real}$: Outlet mass flow field data of the lower line
$\varepsilon$: The hydrogen blending ratio
$p_l$: The lower line outlet pressure
$Pr$: The compressor unit pressure ratio
$K_p$: The proportional coefficient
$K_i$: The integral coefficient
$K_d$: The differential coefficient
$E_r$: PID controller input error
$A_p$: The impact ratio of the pressure ratio on the outlet pressure
$a_p$: The impact ratio of the pressure ratio on the outlet hydrogen blending ratio
$B_h$: The impact ratio of the hydrogen blending amount on the outlet hydrogen blending ratio
$b_h$: The impact ratio of the hydrogen blending amount on the outlet pressure
$\Delta x_1$: The change value of the outlet pressure
$\Delta x_2$: The change value of the outlet hydrogen blending ratio